Received: 26 October 2016 | Revised: 3 January 2017 | Accepted: 17 January 2017
DOI 10.1002/dac.3299

RESEARCH ARTICLE

WILEY

Integrated load-based power saving for real-time and nonreal-time traffic in LTE-TDD

Chun-Chuan Yang[1] | Jeng-Yueng Chen[2] | Yi-Ting Mai[3] | Zheng-Ying Pan[1]

[1] Department of Computer Science and Information Engineering, National Chi Nan University, Puli, Nantou County, Taiwan, R.O.C

[2] Department of Information Networking Technology, Hsiuping University of Science and Technology, Taichung City, Taiwan, R.O.C

[3] Department of Sport Management, National Taiwan University of Sport, Taichung City, Taiwan, R.O.C

Correspondence
Jeng-Yueng Chen, Department of Information Networking Technology, Hsiuping University of Science and Technology, Taichung City, Taiwan, R.O.C.
Email: jychen@ieee.org

Funding information
Ministry of Science and Technology, Taiwan, R.O.C., Grant/Award Number: 104-2221-E-260-004.

Summary

Long-Term Evolution (LTE) is a 4G wireless broadband technology developed by the Third Generation Partnership Project. Two duplex modes, namely, frequency division duplex and time division duplex (TDD), are defined in LTE for transmission in both downlink and uplink directions simultaneously. Power saving mechanisms for LTE-frequency division duplex were proposed in the authors' previous work. Applicability of the previously proposed mechanisms to LTE-TDD is investigated in this paper, and the idea of "virtual time" associated with the mapping mechanism from the virtual time domain to the actual time domain for different TDD configurations is proposed. With the help of the mapping mechanism, 3 revised power saving schemes are proposed to support real-time user equipments and nonreal-time user equipments in LTE-TDD. Simulation study demonstrates the effectiveness of the mapping mechanism as well as the benefit of the proposed schemes in power saving efficiency and real-time support in comparing with the standard-based mechanism.

KEYWORDS
DRX, LBPS, LTE TDD, Power Saving

1 | INTRODUCTION

The advances made in the development of fourth generation cellular networks allow people to interact directly with people from all over the world, creating a more global society. As a major fourth generation system, Long-Term Evolution (LTE)[1] and its enhanced version of LTE-Advanced[2] are being deployed around the world and phasing out 2G and 3G cellular radio methods. Long-Term Evolution is designed to work with a variety of different bandwidths and to deliver a peak data rate of 100 Mbps in the downlink (DL) and 50 Mbps in the uplink (UL), in which the UL is defined for the transmission from the user equipment (denoted by UE) to the base station (denoted by eNodeB) and the DL is defined for the transmission from eNodeB to UE. To be able to transmit in both directions, we find that a UE or eNodeB must have a duplex scheme. There are 2 forms of duplex defined in LTE, namely, frequency division duplex (FDD) and time division duplex (TDD).[3,4]

Frequency division duplex implies that DL and UL transmission take place in different, sufficiently separated, frequency bands. In the case of TDD, there is a single frequency band so that the UL transmission and the DL transmission are separated in the time domain on a cell basis. Different asymmetries in the amount of resources, ie, subframes, allocated for UL and DL transmissions, are provided through the 7 different DL/UL configurations within a radio frame (10 ms) as displayed in Table 1. The switch between DL and

1. Part of the research work in this paper has been published in proceedings of 2016 World Conference on Innovation, Engineering, and Technology (IET 2016), June 24 to 26, 2016, Sapporo, Japan.
2. This work was supported in part by the Ministry of Science and Technology, Taiwan, R.O.C., under grant no. MOST 104-2221-E-260-004.

TABLE 1 TDD configuration

DL/UL Configuration	Subframe Number 0	1	2	3	4	5	6	7	8	9
0	D	S	U	U	U	D	S	U	U	U
1	D	S	U	U	D	D	S	U	U	D
2	D	S	U	D	D	D	S	U	D	D
3	D	S	U	U	U	D	D	D	D	D
4	D	S	U	U	D	D	D	D	D	D
5	D	S	U	D	D	D	D	D	D	D
6	D	S	U	U	U	D	S	U	U	D

Abbreviations: DL, downlink; TDD, time division duplex; UL, uplink. D, DL subframe; U, UL subframe; S, Special subframe.

UL occurs in the special subframe (denote by S in Table 1), which is split into 3 parts: a DL part, a guard period, and a UL part. The DL part can be treated as a DL subframe that can be used to transmit a smaller amount of data than a regular subframe. The UL part, however, is not used for data transmission because of the very short duration. Instead, it can be used for channel sounding or random access. It can also be left empty, in which case it serves as extra guard period.

In this paper, the issue of power saving in LTE-TDD is addressed. The authors have been researching power saving mechanisms in wireless communication systems for some years. The idea of Load-Based Power Saving (LBPS) and associated schemes were proposed for Institute of Electrical and Electronics Engineers 802.16. Load-Based Power Saving schemes for UE power saving in LTE-FDD were also proposed in the authors' previous work. In order for the previously proposed schemes to be applied to LTE-TDD, the idea of virtual time associated with the mapping mechanism from the virtual time to the actual time is proposed in this paper, and 3 revised versions of LBPS schemes to integrate real-time (RT) and nonreal-time (NRT) traffic in sleep scheduling are proposed. Note that the term “actual time,” instead of “real time,” is used as the contrast of “virtual time” to avoid ambiguity with “real time” that is used to associate traffic with bounded transmission delays.

The remainder of the paper is organized as follows. In Section 2, a brief survey of LTE-TDD–related research and authors' previous work of LBPS is presented. Proposed schemes for power saving in LTE-TDD, including the mapping mechanism and integrated sleep scheduling schemes for RT and NRT traffic, are presented in Section 3. Performance evaluation is presented in Section 4. Finally, Section 5 concludes this paper.

2 | RELATED WORK

2.1 | LTE-TDD–related research

LTE-TDD–related research in the literature can be classified into the following categories: (1) performance issue of the HARQ (Hybrid Automatic Repeat Request) operation, (2) resource allocation and DL/UL reconfiguration, and (3) interference mitigation, as briefly surveyed in the following.

In a dynamic TDD system, the DL/UL configuration can be changed on the basis on the traffic load, which leads to the performance issue of HARQ operation. An implementation of DL asynchronous HARQ that the eNodeB can apply for the TDD configuration in minimize the retransmission time was proposed in 1 study.[5] To reduce the signaling overhead in Physical Uplink Control Channel and increase the spectrum efficiency, the authors of previous study[6] designed 2 novel HARQ feedback signaling schemes. In the case of Machine Type Communications in LTE-TDD, the problem of the large number of HARQ ACK/NACKs for different DL subframes transmitted in a given UL subframe was addressed in this study,[7] in which a novel scheme combining multiple HARQ ACK/NACKs into an ACK/NACK was proposed to decrease the number of transmissions. In the work of Lu et al,[8] a low latency DL HARQ feedback method for TDD Carrier Aggregation systems is proposed to shorten the transmission delay.

The issue of resource allocation in dynamic TDD is concerning about dynamic DL/UL reconfiguration to adapt to different traffic types as well as the load condition. To meet the requirement that all cells in the network follow the same TDD UL/DL configuration for interference mitigation, the authors of previous study[9] proposed a distributed algorithm to determine the optimum configuration according to the available UL and DL traffic of all radio resource control–connected UEs in different cells within the network. The case of the UL traffic much higher than DL traffic in smart grid communications was analyzed in 1 study[10] to find the best TDD configuration in the average UL latency.

Intercell interference among neighboring cells adopting TDD dynamic UL/DL reconfiguration imposes severe performance problem, since having different UL/DL directions for the same subframe in adjacent cells can result in new destructive interference components, ie, eNodeB-to-eNodeB interference and UE-to-UE interference. The idea of transmission power control for interference mitigation was proposed in previous studies.[11,12] The authors demonstrated that by reducing the transmission power in DL subframes causing eNodeB-to-eNodeB interference, and by boosting the transmission power in UL subframes suffering eNodeB-to-eNodeB interference, UL throughput can be improved without significant DL throughput degradation. Authors of other literature[13,14] focused on a particular small cell architecture, namely, the Phantom Cell architecture, adopted the technique of frequency reuse to mitigate intercell interference, and proposed a half-duplex FDD-like radio resource assignment technique, which is a hybrid combination of TDD and FDD.

2.2 | Previous work of LBPS

The basic idea of LBPS is to use the technique of traffic modelling in determining the length of the sleep period. The traffic in LBPS is assumed to be Poisson process to take advantage of the multiplexing property. The eNodeB estimates the traffic load and calculates the length of the sleep period in order for the accumulated data in the eNodeB's buffer reaching a predefined level denoted by Data_TH in LBPS. Three LBPS schemes, namely, LBPS-Aggr, LBPS-Split, and LBPS-Merge, were proposed to deal with multiplexing UEs in sleep scheduling. LBPS-Aggr is the simplest scheme that treats all traffic as an aggregate flow in determining the length of the sleep period and synchronizes all UEs in sleep scheduling. The other 2 enhanced LBPS schemes try to lengthen the sleep period by making UEs into different groups in sleep scheduling. Starting from the same position as LBPS-Aggr, LBPS-Split tries to split the UEs into more groups until there is no space for further splitting. Taking the reverse direction of LBPS-Split, LBPS-Merge initially treats each UE as a single-member group and merges some of the groups until a feasible sleep schedule is found. The cycle length for each group in LBPS-Merge is converted the closest and smaller power of 2 to efficiently find a feasible sleep schedule for all groups. Please refer to the authors' previous work[15,16] for more details of the LBPS schemes.

3 | LBPS INTEGRATING RT AND NRT IN TDD

Based on the previous work, the extended work of LBPS to support RT and NRT traffic in LTE-TDD is proposed in this paper. Since the previous work was proposed only for NRT in LTE-FDD, there are 2 parts in the proposed work, ie, TDD supporting and RT supporting, as presented in the following sections.

3.1 | The idea of virtual time for TDD

The LBPS schemes in the authors' previous work were originally designed for LTE-FDD. Although based on the general idea of data accumulation according to the estimated input load and the estimated capacity in a subframe, sleep schedule in the schemes were assigned by assuming the availability of every subframe in a continuous manner. Two issues should be addressed to apply the LBPS schemes to LTE-TDD. Firstly, since the availability of subframe for DL data transmission in TDD depends on the given configuration, the algorithm of sleep scheduling needs to consider the pattern of available subframes. Secondly, the calculation of the estimated capacity for data accumulation needs to be revised, since the overall system capacity also depends on the TDD configuration.

There are 2 possible directions to design the algorithm of sleep scheduling in LTE-TDD. The first direction is to redesign a new set of schemes to accommodate different availability patterns of data transmission for different TDD configurations. However, this way would increase the complexity in sleep scheduling especially for a complicated scheme, such as LBPS-Split or LBPS-Merge, which adopts the mechanism of grouping UEs by splitting or merging.

Another direction is adopted by the authors to keep the previous LBPS schemes unchanged as much as possible and operate the schemes in the domain of virtual time, in which every subframe is continuously available for DL transmission. The result of sleep scheduling generated by the LBPS schemes in the domain of virtual time is then mapped to a sleep schedule in the domain of actual time. Therefore, to apply LBPS schemes in LTE-TDD, we proposed the idea of virtual time associated with the mapping mechanisms from virtual time to actual time for different TDD configurations in this paper. Mapping mechanisms for some of the configurations are presented in the next section. Note that the proposed mechanisms and schemes in this paper are according to the given TDD configuration, but the selection of a proper configuration for a given network condition (also known as the issue of dynamic TDD) is beyond the scope of the paper.

3.2 | Mapping mechanisms

Although the system capacity depends on the channel quality, every subframe in virtual time is assumed to have the same amount of radio resource, which is allocated from the available radio resource in actual time. Therefore, the design of the mapping mechanism for a given TDD configuration turns to be the problem of allocating available radio resource to each of the subframe in virtual time. Since this paper focuses on DL traffic, the available radio resource for allocation is those subframes marked as "D" (for DL transmission) in TDD configurations as displayed in Table 1. For the sake of simplicity, the special subframe (marked as "S") is not considered for DL transmission in the paper. Moreover, the capacity of each available subframe in actual time is also assumed to be equal. A subframe in virtual time is called a virtual subframe, and a subframe in actual time is called an actual subframe in the paper.

Taking Configuration 1 (denoted by C1) as an explanatory example, there are 3 possible methods for allocating all available DL radio resources to each virtual subframe in a cycle of 10 ms, which is the length of a radio frame in LTE. The first method is called one-to-all mapping, denoted by M1 in the paper, in which the radio resource for a virtual subframe comes from every available actual subframe. An example illustrating the mapping in a cycle of 10 subframes is given in Figure 1, in which there are 3 parts in the figure: the upper part displays the actual subframes, the middle part displays the virtual subframes, and the lower part indicates the mapping from each virtual subframe to the actual subframe(s). As illustrated in Figure 1, there are 4 actual subframes in a cycle of 10 ms in C1. Each actual subframe contributes 1/10 of its radio resource to each virtual subframe. In this way, each virtual subframe is given 4/10 of the capacity in an actual subframe and maps to actual subframes 0, 4, 5, and 9 in M1, which means an awake virtual subframe (eg, virtual subframe 0) determined by the sleep scheduling scheme results in 4 awake actual subframes (ie, actual subframes 0, 4, 5, and 9). Apparently M1 is not a good way of mapping from the viewpoint of power saving efficiency; thus, it serves as a contrast to other mapping mechanisms.

Another method of mapping is called continuous mapping, denoted by M2. In M2, as illustrated in Figure 2, starting from actual subframe 0 the available radio resource is first allocated to virtual subframe 0 until reaching the equal share of the total capacity, ie, 4/10 of the capacity in an actual subframe in the case of C1. Another 4/10 of the capacity from actual subframe 0 is allocated to virtual subframe 1. The rest of 2/10 of the capacity from actual subframe 0 combined with 2/10 of the capacity from actual subframe 4 (the next available subframe in C1) is then allocated to virtual subframe 2. The rest of the radio resource from actual subframe 4 is allocated to virtual subframes 3 and 4. The allocation process continues until all virtual subframes get their shares of the available radio resource. As displayed in the bottom part of Figure 2, there are only 2 cases of 1-to-2 mapping (1 virtual subframe maps to 2 actual subframes) in M2: virtual subframe 2 to actual subframes 0 and 4 and virtual subframe 7 to actual subframes 5 and 9. The rest of the mapping is all 1-to-1.

The third method is called one-to-one first mapping, denoted by M3. As illustrated in Figure 3, M3 makes 1-to-1 mapping first and combines the rest of the radio resource for allocation. In this way, the type of 1-to-1 mapping from virtual to actual (virtual subframe 0 ~ 7) goes first followed by the type of 1-to-2 mapping (virtual subframe 8 ~ 9) in M3. Moreover, as in M2, there are also 2 cases of 1-to-2 mapping in M3 for C1, and the difference is that the cases in M3 are next to each other (virtual subframes 8 and 9).

The upper part of Table 2 displays C1's 3 mappings, denoted by C1M1, C1M2, and C1M3. The entry in the row of a mapping in the table displays the actual subframe number(s) to which the intended virtual subframe is mapping. For instance, the first entry of C1M1 shows that virtual subframe 0 maps to actual subframes 0, 4, 5, and 9. The mappings for another 2 configurations, C3 and C5, are also included in the table. Note that a significant difference between C5M2 and C5M3 lies in the number of 1-to-many mapping. There are 6 cases of 1-to-2 mapping in C5M2. However, except the 2 cases of 1-to-4 mapping in C5M3, the rest is all 1-to-1. The impact of the number of 1-to-many mapping on the performance of power saving is investigated in Section 4.

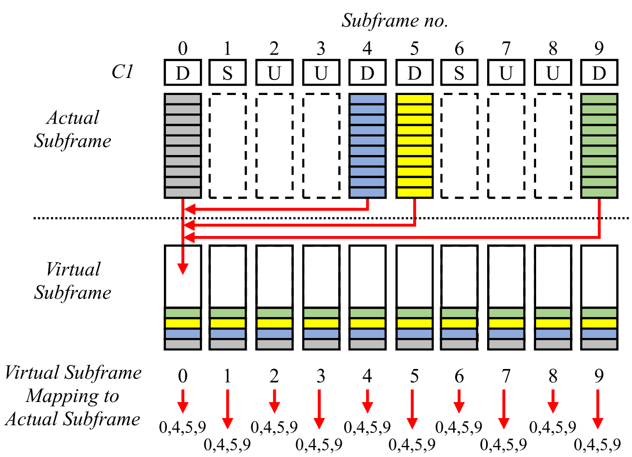

FIGURE 1 One-to-all mapping (M1) for C1

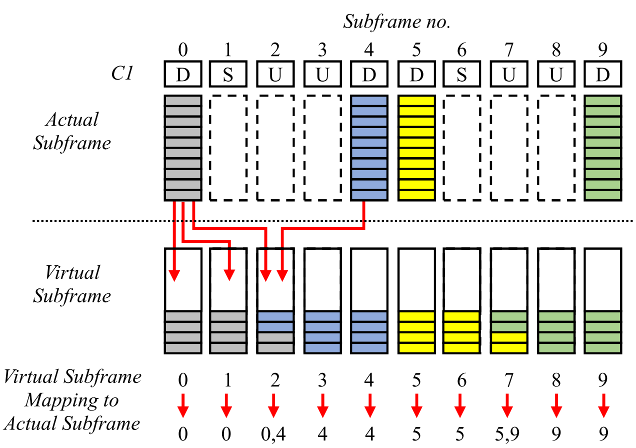

FIGURE 2 Continuous mapping (M2) for C1

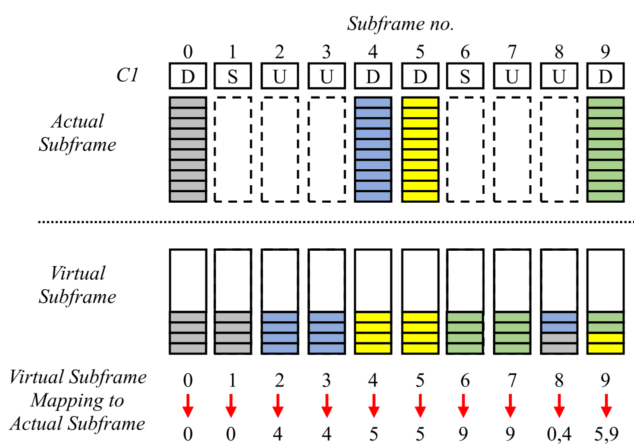

FIGURE 3 One-to-one first mapping (M3) for C1

TABLE 2 Mapping for C1, C3, and C5

Configuration Mapping	Subframe Number									
	0	1	2	3	4	5	6	7	8	9
C1	D	S	U	U	D	D	S	U	U	D
C1M1	0,4 5,9	0,4 5,9	0,4 5,9	0,4 5,9	0,4 5,9	0,4 5,9	0,4 5,9	0,4 5,9	0,4 5,9	0,4 5,9
C1M2	0	0	0,4	4	4	5	5	5,9	9	9
C1M3	0	0	4	4	5	5	9	9	0,4	5,9
C3	D	S	U	U	U	D	D	D	D	D
C3M1	0, 5 ~ 9	0, 5 ~ 9	0, 5 ~ 9	0, 5 ~ 9	0, 5 ~ 9	0, 5 ~ 9	0, 5 ~ 9	0, 5 ~ 9	0, 5 ~ 9	0, 5 ~ 9
C3M2	0	0,5	5	5,6	6	7	7,8	8	8,9	9
C3M3	0	5	6	7	8	9	0,5	5,6	7,8	8,9
C5	D	S	U	D	D	D	D	D	D	D
C5M1	0, 3 ~ 9	0, 3 ~ 9	0, 3 ~ 9	0, 3 ~ 9	0, 3 ~ 9	0, 3 ~ 9	0, 3 ~ 9	0, 3 ~ 9	0, 3 ~ 9	0, 3 ~ 9
C5M2	0	0,3	3,4	4,5	5	6	6,7	7,8	8,9	9
C5M3	0	3	4	5	6	7	8	9	0, 3 ~ 5	6 ~ 9

3.3 | RT support

With the help of the proposed mapping mechanisms, the previous LBPS schemes can be applied to LTE-TDD. In this section, 3 revised LBPS schemes, namely, LBPS-Aggr-RT, LBPS-Split-RT, and LBPS-Merge-RT, are proposed for RT support in bounded delays. Two factors need to be considered in designing the revised schemes for RT support in LTE-TDD: delays created by sleep scheduling and delays created by the mapping mechanisms. According to the design of LBPS schemes, the delays created by sleep scheduling are bounded by the length of the sleep cycle for a UE, which means that the given delay bound (DB) for a UE should be taken into consideration in sleep scheduling. On the other hand, the delay is also increased by the time offset from virtual time to actual time in the mapping mechanisms. Therefore, the maximum offset caused by the mapping mechanisms should also be taken into consideration in sleep scheduling. Table 3 displays the maximum offset (denoted by MaxOffset) of different mappings for configuration C1, C3, and C5. For instance, the maximum offset (ie, 9 ms) in C1M1 occurs in the case that virtual subframe 0 maps to actual subframe 9, and MaxOffset = 2 ms in C1M2 occurs in the case that virtual subframe 2 maps to actual subframe 4 and virtual subframe 7 maps to actual subframe 9 as well.

Overview of the proposed RT sleep scheduling in LTE-TDD is displayed in Figure 4. As illustrated in Figure 4, the value of Data_TH is calculated according to the estimated capacity of a subframe and the given TDD configuration. The estimated load, DBs, the value of Data_TH, and the maximum mapping offset according to the TDD configuration are fed into the sleep scheduling scheme to generate a virtual sleep schedule, which is further converted to an actual sleep schedule by the mapping mechanism. Lastly, eNodeB notifies related UEs by transmitting the message of Radio Resource Control Connection Configuration.

Notations used in the proposed schemes are listed as follows:

λ_i	the estimated DL load for UE_i
DB_i	the given DB for UE_i (Note that $DB_i = \infty$ for an NRT UE)
DB_{min}	the minimum DB among the UEs in the same group in sleep scheduling
$C_{Channel}$	the estimated channel capacity for UEs in the group for the given TDD configuration

Since the proposed schemes are operated in the domain of virtual time, the calculation of $C_{Channel}$ depends on the capacity of a DL subframe as well as the ratio of DL subframes in a radio frame. For example, the ratio of DL subframes in C1 is 4/10, and $C_{Channel}$ = (Estimated Capacity in a DL subframe) × 0.4. In the following, the 3 proposed LBPS schemes for RT support in LTE-TDD are presented.

3.3.1 | LBPS-Aggr-RT

Since all UEs are grouped together in sleep scheduling in LBPS-Aggr-RT, revision of the scheme is simpler than the

TABLE 3 Maximum offset of different mappings for C1, C3, and C5

Configuration Mapping	MaxOffset, ms	Remark
C1M1	9	virtual subframe 0 maps to actual subframe 9
C1M2	2	virtual subframe 2 maps to actual subframe 4 virtual subframe 7 maps to actual subframe 9
C1M3	3	virtual subframe 6 maps to actual subframe 9
C3M1	9	virtual subframe 0 maps to actual subframe 9
C3M2	4	virtual subframe 1 maps to actual subframe 5
C3M3	4	virtual subframe 1 maps to actual subframe 5 virtual subframe 2 maps to actual subframe 6 ...
C5M1	9	virtual subframe 0 maps to actual subframe 9
C5M2	2	virtual subframe 1 maps to actual subframe 3 virtual subframe 2 maps to actual subframe 4 virtual subframe 3 maps to actual subframe 5
C5M3	2	virtual subframe 1 maps to actual subframe 3 virtual subframe 2 maps to actual subframe 4 ...

other 2 schemes. There are mainly 3 steps to determine the next sleep cycle in the scheme as presented in the following:

Step 1. Calculating the length of the sleep cycle according to the estimated load.

$$K = LengthAwkSlpCyl\,(\lambda, Data\_TH), \text{ where } \lambda = \Sigma_i \lambda_i, \text{ and } Data\_TH = \alpha \times C_{Channel}. \quad (1)$$

Please refer to the authors' previous work[16] for the calculation of function *LengthAwkSlpCyl*. Note that the threshold of data accumulation Data_TH is set as a percentage (α) of the capacity to reduce the probability that the amount of data exceeding the capacity (α = 0.8 in the simulation).

Step 2. Adjusting the length of the sleep cycle according to the minimum DB and the maximum offset caused by the mapping mechanism.

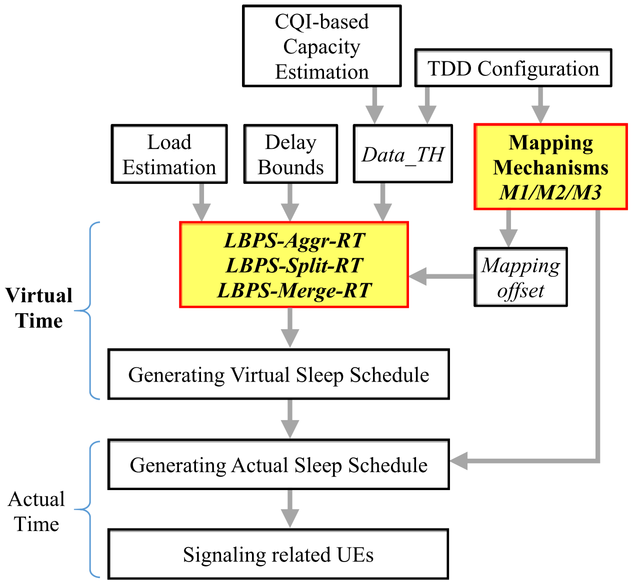

FIGURE 4 Real-time sleep scheduling in Long-Term Evolution–time division duplex

$$K^* = \text{Min}\,(K, DB_{min} - MaxOffset), \text{ where } DB_{min} = \text{Min}\,(DB_i) \text{ for all } UE_i. \quad (2)$$

Step 3. Generating the sleep schedule with the cycle length K^* in virtual time, and through the mapping mechanism, making the actual sleep schedule and notifying the related UEs.

3.3.2 | LBPS-Split-RT

The basic idea of LBPS-Split-RT is through the operation of splitting UEs into different groups in sleep scheduling; the length of the sleep cycle can be increased and therefore to achieve higher power saving efficiency. The first iteration in LBPS-Split-RT is the same as the operation of LBPS-Aggr-RT. If the calculated length of the sleep cycle in the first iteration is larger than 1 (subframe), a series of splitting process is performed. With both RT UEs and NRT UEs in the network, it is intuitively to separate RT UEs and NRT UEs in different groups. However, since the same cycle length derived from the minimum cycle length among all groups is used for all groups in LBPS-Split-RT, meaning that the DB of any RT UE will eventually affect the length of the sleep cycle, there is no need to separate RT UEs and NRT UEs in sleep scheduling. Hence, the goal of the splitting mechanism in LBPS-Split-RT is to minimize the difference of load among groups. Major steps in LBPS-Split-RT are presented in the following:

Step 1. Calculating the cycle length for the first iteration, in which all UEs (RT + NRT) in one group.

$$K = LengthAwkSlpCyl(\lambda, Data\_TH), where \quad \lambda = \sum_i \lambda_i, \text{ and } Data\_TH = \alpha \times C_{Channel}, \tag{3}$$

$$K^* = \text{Min } (K, DB_{min} - MaxOffset), \text{ where } \quad DB_{min} = \text{Min } (DB_i) \text{ for all } UE_i. \tag{4}$$

Step 2. Splitting UEs to increase K^*.
If $K^* > 1$, splitting all UEs into K^* groups, and

1. For each group G_i, calculate its cycle length K^*_{Gi} as follows:

$$K_{Gi} = LengthAwkSlpCyl\ (\lambda, Data\_TH), \text{ where } \quad \lambda = \sum_{UE_m \in G_i} \lambda_m, \tag{5}$$

$$K^*_{Gi} = \text{Min } (K_{Gi}, DB_{min} - MaxOffset), \text{ where } \quad DB_{min} = \text{Min } (DB_m) \text{ for all } UE_m \in G_i. \tag{6}$$

2. The cycle length of the iteration is calculated as the minimum length among all K^* groups:

$$\text{Set } new\ K^* = \text{the smallest one among } K^*_{Gi}$$

3. Check the possibility for more splitting:
   If the *new* K^* is the same as the one in the previous iteration, go to Step 3.
   Else repeat Step 2.

Else go to Step 3.

Step 3. Generating the sleep schedule in virtual time according to final K^*, and through the mapping mechanism, making the actual sleep schedule and notifying the related UEs.

3.3.3 | LBPS-Merge-RT

Starting from each UE forming a single-member group, LBPS-Merge-RT allows UEs to have different cycle lengths in the sleep schedule. The cycle length calculated by the function of LengthAwkSlpCyl and the delay bound DB_i for each UE is converted to the closest and smaller power of 2 to simplify schedulability check. If it is failed to find a feasible schedule, a series of merge operation is performed until the check of schedulability is passed. The following 2 strategies are adopted in the merge operation.

1. Separating RT UEs and NRT UEs in different groups, unless there is no other choice.
2. Minimizing the reduction of power saving efficiency in the merge operation, in which 2 types of merge were defined in the previous work, nondegraded merge and degraded merge. The merge of 2 groups that does not result in a smaller cycle length is called a nondegraded merge. A degraded merge is performed only when a nondegraded merge cannot be found.
   Major steps in LBPS-Merge-RT are presented in the following:

Step 1. Calculating the cycle length for the first iteration, in which each UE forms a group.
In general, the cycle length for group G_i is calculated as follows:

$$K_{Gi} = LengthAwkSlpCyl\ (\lambda_{Gi}, Data\_TH), \text{ where } \quad \lambda_{Gi} = \text{the total load in group } G_i, \text{ and } \quad Data\_TH = \alpha \times C_{Channel}, \tag{7}$$

$$K^*_{Gi} = \text{Min } (K_{Gi}, DB_{Gi} - MaxOffset), \text{ where } \quad DB_{Gi} = \text{Min } (DB_m) \text{ for all } UE_m \in G_i, \tag{8}$$

$$K^{\#}_{Gi} = 2^{\lfloor \log_2 K^*_{Gi} \rfloor}, \tag{9}$$

$$Schedulability = \sum_{Gi} \frac{1}{K^{\#}_{Gi}}. \tag{10}$$

If *Schedulability* < = 1, go to Step 3 (ie, a feasible sleep schedule can be found).
Else go to Step 2 (to start the merge process).

Step 2. According to the aforementioned 2 strategies for merge operation, merging the 2 groups with the smallest cycle length, recalculating the cycle length of the new group according to the calculation in Step 1.

If the new value of *Schedulability* < = 1, go to Step 3 (ie, a feasible sleep schedule can be found).
Else repeat Step 2 (for another merge operation).

Step 3. Generating the sleep schedule in virtual time according to the final set of $K^{\#}_{Gi}$, and through the mapping mechanism, making the actual sleep schedule and notifying the related UEs.

4 | PERFORMANCE EVALUATION

In this section, a performance comparison by theoretical analysis in power saving efficiency for 3 different mapping mechanisms is presented, followed by the results of the simulation study. The following criteria are defined for performance evaluation and comparison:

1. Power saving efficiency, denoted by PSE, is defined as the ratio of time for UEs in the sleep mode.
2. Average delay, denoted by AvgDelay, is defined as the average access delay of packets. AvgDelay for RT and NRT traffic is calculated separately in the simulation.
3. Packet loss ratio, denoted by PLR, is defined as the percentage of discarded RT packets due to exceeding the corresponding DB.

4.1 | Theoretical analysis of the mapping mechanisms

To investigate the impact of the mapping mechanism on power saving, we investigated the relationship between PSE in virtual time (denoted by $PSE_{Virtual}$) and PSE in actual time (denoted by PSE_{Actual}) for different mapping mechanisms. Considering the case of $PSE_{Virtual} = 0.9$ as an example, in which on the average, there is 1 awake virtual subframe within 10 ms. We assume that each virtual subframe within a radio frame has the equal probability (ie, 1/10) to be the awake subframe. Therefore, the average value of PSE_{Actual} can be calculated as follows: (Note that *sf* is the abbreviation for subframe in the equation)

$$\mathrm{PSE}_{\mathrm{Actual}} = \frac{1}{10}\sum_{i=0}^{9}\left(1-\frac{\text{No.of } \textit{mapped actual sf} \text{ for } \textit{virtual sf i}}{10}\right). \tag{11}$$

The value of PSE_{Actual} for $PSE_{Virtual} = 0.9$ in different configurations and mappings is displayed in Table 4. In the same way, the value of PSE_{Actual} for different $PSE_{Virtual}$ can be derived. Figure 5 displays the relationship between $PSE_{Virtual}$ and PSE_{Actual} for different mapping mechanisms. Some observations can be made according to the figure. First of all, as expected, the method of M1 mapping results in the smallest value of PSE_{Actual}. Secondly, the same value of PSE_{Actual} in M2 and M3 for a configuration implies that M2 and M3 have similar power saving performance. However, as will be demonstrated in the simulation study, M3 outperforms M2 in most cases.

4.2 | Simulation results for NRT only

To investigate the impact of the mapping mechanisms associated with the proposed LBPS schemes on PSE, we considered the case that only NRT UEs are present in the network in this section. Three types of UEs are defined for simulating different cases of the channel quality. An H-type (high link quality) UE is assumed to use 64 quadrature amplitude modulation with channel quality indicator (CQI) value ranging from 10 to 15. An M-type (medium link quality) UE uses 16 quadrature amplitude modulation with CQI ranging from 7 to 9. An L-type (low link quality) UE uses quadrature phase shift keying with CQI ranging from 1 to 6. In addition to the 3 proposed LBPS schemes, a contrast scheme based on standard Discontinuous Reception (DRX) (denoted by *Std. DRX*) is also simulated. Parameters used in the simulation are summarized in Table 5.

TABLE 4 PSE_{Actual} for $PSE_{Virtual} = 0.9$

Mapping	PSE_{Actual}	Remarks
C1M1	0.6	1-to-4 × 10
C1M2	0.88	1-to-1 × 8, 1-to-2 × 2
C1M3	0.88	1-to-1 × 8, 1-to-2 × 2
C3M1	0.4	1-to-6 × 10
C3M2	0.86	1-to-1 × 6, 1-to-2 × 4
C3M3	0.86	1-to-1 × 6, 1-to-2 × 4
C5M1	0.2	1-to-8 × 10
C5M2	0.84	1-to-1 × 4, 1-to-2 × 6
C5M3	0.84	1-to-1 × 8, 1-to-4 × 2

Abbreviation: PSE, Power Saving Efficiency

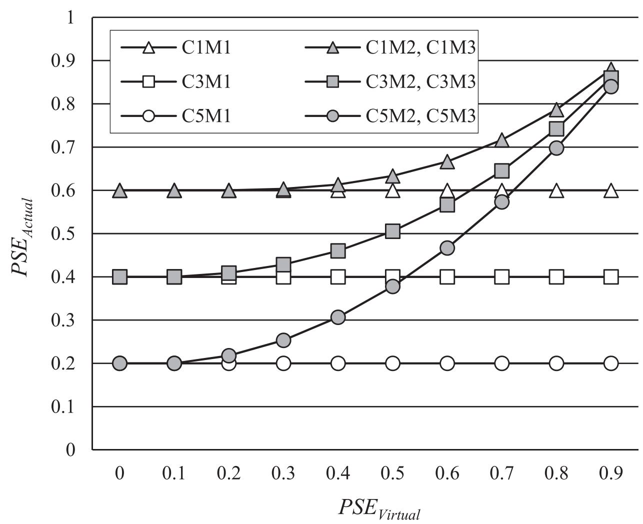

FIGURE 5 Comparison of the mapping mechanisms. PSE, Power Saving Efficiency

Figures 6–8 display the results of PSE for different mappings in the scheme of LBPS-Aggr-RT with All-H type UEs. In the figures, there are 2 rows of index for the x-axis. The upper row is the input load λ in Mbps, and the lower row is the normalized utilization ρ calculated as dividing the input load by the average system capacity. As expected, the mapping of M1 results in the worst PSE among the mapping mechanisms.

TABLE 5 Simulation parameters

Parameter	Value
Channel capacity	20 MHz (#RB = 100)
No. of UE	40 (equal load)
Type of UE	H-type: CQI 10 ~ 15 M-type: CQI 7 ~ 9 L-type: CQI 1 ~ 6
Packet size	799 bits
DATA_TH	Estimated capacity × Prob_TH
Prob_TH	0.8
Min. group size	1
Contrast scheme *Std. DRX*	On duration = 1 ms Inactivity timer = 10 ms Short DRX cycle = 40 ms Short cycle timer = 2 ms Long DRX cycle = 160 ms

Abbreviations: CQI, channel quality indicator; UE, user equipment.

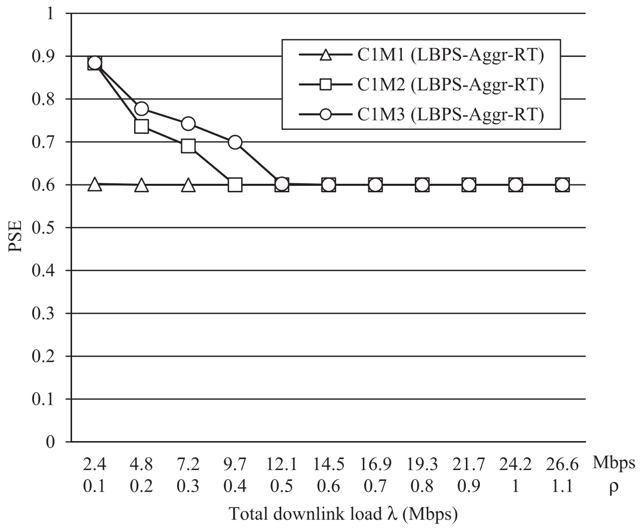

FIGURE 6 PSE of different mappings for C1 (All-H UEs). LBPS, Load-Based Power Saving; PSE, power saving efficiency; RT, real-time; UE, user equipment

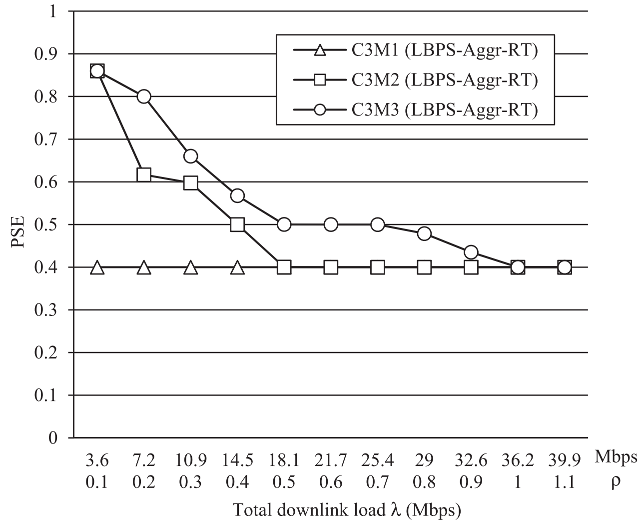

FIGURE 7 PSE of different mappings for C3 (All-H UEs). LBPS, Load-Based Power Saving; PSE, power saving efficiency; RT, real-time; UE, user equipment

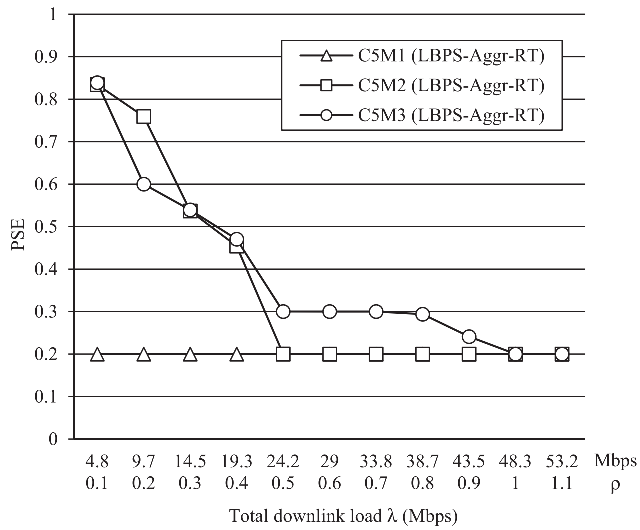

FIGURE 8 PSE of different mappings for C5 (All-H UEs). LBPS, Load-Based Power Saving; PSE, power saving efficiency; RT, real-time; UE, user equipment

On the other hand, although with the same analytical PSE result (as displayed in Table 4) and similar simulation results for $\rho = 0.1$, M3 outperforms M2 in most of the load cases. The reason lies in the assumption of the equal probability for each virtual subframe to be the awake subframe in the analysis. The assumption of equal probability holds for the light load of $\rho = 0.1$, which is demonstrated by the simulation results. However, the assumption no longer holds when ρ is larger than 0.1, and in most of the cases, the clustering behavior of 1-to-many mappings in M3 creates more benefit than the scattering style of M2 in PSE.

Figures 9–11 display the results of PSE for different schemes with All-H type UEs using the best mapping of M3. The figures show that in PSE, the schemes of LBPS-Split-RT and LBPS-Merge-RT outperform the scheme of LBPS-Aggr-RT, which outperforms the contrast scheme of *Std. DRX*, demonstrating the benefit of the proposed schemes in power saving. Moreover, there is no significant difference in PSE for LBPS-Split-RT and LBPS-Merge-RT, except in some cases of pretty heavy load such as $\rho = 0.9$ in Figures 10 and 11. Note that the benefit of LBPS-Merge-RT over LBPS-Split-RT in PSE is to allow different cycle lengths in sleep scheduling at the cost of reducing the length to a power of 2 for schedulability. Better PSE for LBPS-Merge-RT in the cases of $\rho = 0.9$ in Figures 10 and 11 demonstrates the

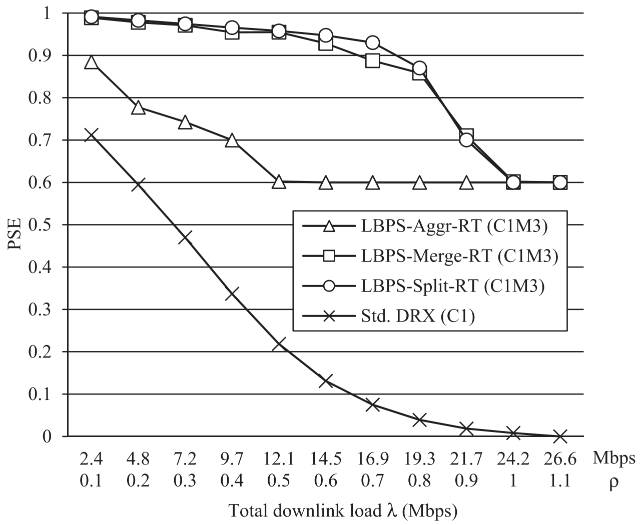

FIGURE 9 *PSE* of different schemes for *C1* (All-H UEs). LBPS, Load-Based Power Saving; PSE, power saving efficiency; RT, real-time; UE, user equipment

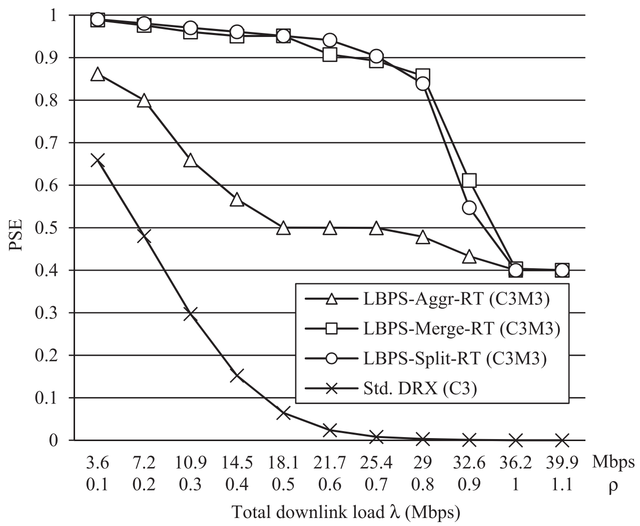

FIGURE 10 PSE of different schemes for C3 (All-H UEs). LBPS, Load-Based Power Saving; PSE, power saving efficiency; RT, real-time; UE, user equipment

benefit of allowing different cycle lengths. However, there are also cases (such as ρ = 0.6 in Figures 9–11) that the benefit of different cycle lengths is compromised by the cost of reducing the length to a power of 2, making LBPS-Merge-RT achieve slightly smaller PSE than LBPS-Split-RT.

4.3 | Simulation results for RT + NRT

In this section, both RT UEs and NRT UEs are present in the simulated network. Simulation parameters are the same as in Table 5, and the number of RT UEs and the number of NRT UEs are equal (ie, 20 RT UEs and 20 NRT UEs).

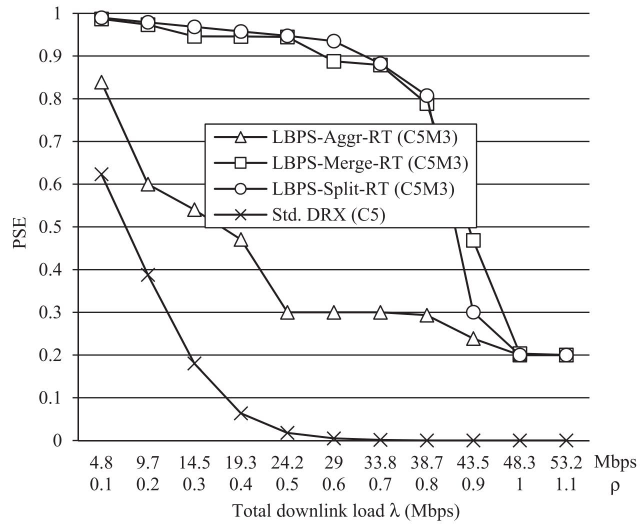

FIGURE 11 PSE of different schemes for C5 (All-H UEs). LBPS, Load-Based Power Saving; PSE, power saving efficiency; RT, real-time; UE, user equipment

The value of DB for each RT UE is the same, and 3 DB values (25, 12, and 6 ms) are simulated, respectively. In addition, the simulation assumes that RT packets have priority over NRT packets in transmission scheduling. Since the contrast scheme of *Std. DRX* lacks of the ability to support RT and LBPS-Aggr-RT is essentially inferior to the other proposed schemes in RT support, only results of LBPS-Split-RT and LBPS-Merge-RT are displayed in this section.

Figures 12 and 13 display NRT's PSE and RT's PSE, respectively, for C3 using M3 mapping mechanism. Some observations from the figures can be made as follows:

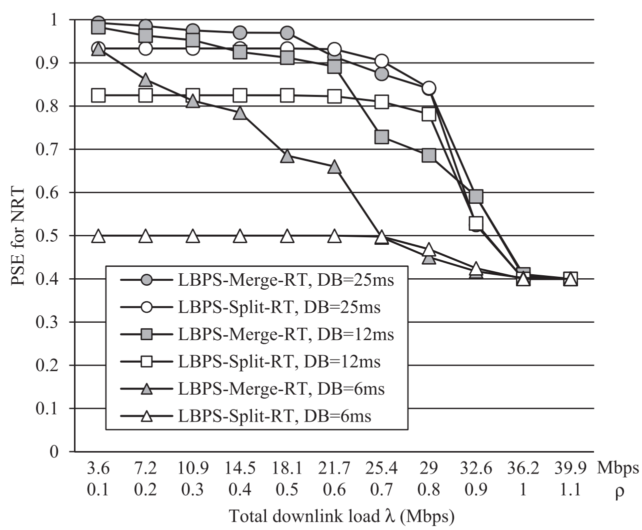

FIGURE 12 PSE for NRT in C3 (All-H UEs). DB, delay bound; LBPS, Load-Based Power Saving; NRT, nonreal-time; PSE, power saving efficiency; RT, real-time; UE, user equipment

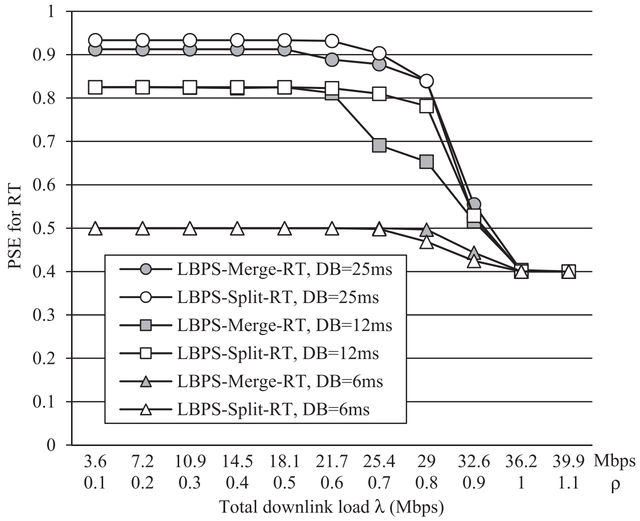

FIGURE 13 PSE for RT in C3 (All-H UEs). DB, delay bound; LBPS, Load-Based Power Saving; PSE, power saving efficiency; RT, real-time; UE, user equipment

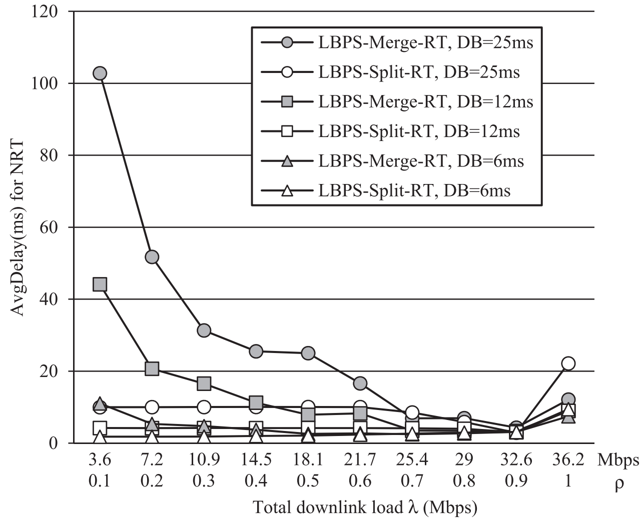

FIGURE 14 AvgDelay for NRT in C3 (All-H UEs). DB, delay bound; LBPS, Load-Based Power Saving; NRT, nonreal-time; RT, real-time; UE, user equipment

1. A smaller value of DB for RT UEs results in smaller RT's PSE as well as NRT's PSE, since a smaller DB value imposes a tighter constraint on sleep cycle length for some groups in LBPS-Merge-RT and for all groups in LBPS-Split-RT. Moreover, as the load increases, the sleep cycle length becomes smaller, which dilutes the impact of the DB value on PSE. Therefore, all curves of RT's PSE and NRT's PSE converge at pretty heavy loads ($\rho > 0.9$).
2. When the input load is not too heavy ($\rho < 0.7$), LBPS-Merge-RT outperforms LBPS-Split-RT in NRT's PSE because of the flexibility of LBPS-Merge-RT by allowing different cycle lengths in sleep scheduling.
3. RT's PSE is equal to NRT's PSE in LBPS-Split-RT, since RT UEs and NRT UEs share the same cycle length in sleep scheduling in LBPS-Split-RT. There is no significant difference in RT's PSE between LBPS-Split-RT and LBPS-Merge-RT, except for the cases of $\rho = 0.7$ and 0.8 under DB = 12 ms in Figure 13, in which the cost of reducing the cycle length to a power of 2 for schedulability in LBPS-Merge-RT results in greater loss in RT's PSE (also in NRT's PSE as shown in Figure 12).

Figures 14 and 15 display the results of AvgDelay for NRT and RT, respectively. Note that the case of $\rho = 1.1$ for NRT is not displayed in Figure 14 since the values of AvgDelay for $\rho = 1.1$ are too large (over 450 ms) in comparison with other loads. Moreover, since the RT packets not transmitted within the time of the corresponding DB are discarded in the simulation, the value of AvgDelay for RT in Figure 15 does not include all incoming RT packets. The following observations can be made from Figures 14 and 15:

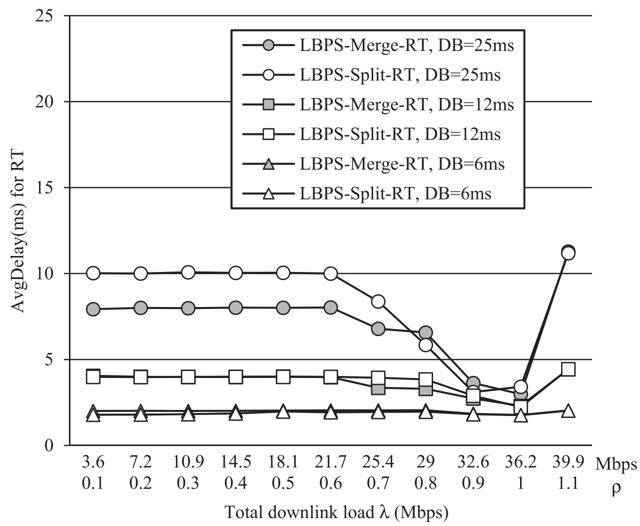

FIGURE 15 AvgDelay for RT in C3 (All-H UEs). DB, delay bound; LBPS, Load-Based Power Saving; RT, real-time; UE, user equipment

1. LBPS-Merge-RT can effectively separate NRT and RT in sleep scheduling, making clear distinction between NRT's AvgDelay and RT's AvgDelay (ie, NRT's AvgDelay is much higher than RT's AvgDelay). On the other hand, there is no significant difference in NRT's and RT's AvgDelay for LBPS-Split-RT.
2. As will be shown in the following results of PLR, most of the RT packets can be transmitted within corresponding DB in both schemes. For the lower value of RT's AvgDelay under DB = 25 ms in LBPS-Merge-RT than LBPS-Split-RT, the reason is due to the reduced cycle length in LBPS-Merge-RT by converting the cycle length to a power of 2.

Figures 16 and 17 display the results of PLR for RT packets under DB = 6 ms and DB = 12 ms, respectively. Note that the result of PLR under DB = 25 ms is not displayed in the paper since PLR for the case is pretty small in both schemes. The following observations can be made from Figures 16 and 17:

1. When the input load is not too heavy ($\rho < 1$), there is some space for RT UEs to enter the sleep mode in both schemes. Although the 2 schemes are designed to limit the sleep cycle length smaller than the DB, the stochastic nature of the arrival processes still results in cases that some RT packets cannot be transmitted within the corresponding DB. However, the value of PLR for both schemes is mostly under 3% when $\rho < 1$, which should be acceptable for most multimedia applications. If PLR is to be reduced further, the sleep cycle length in both schemes should be reduced by assigning a lower value of Data_TH.
2. For the case of the input load $\rho = 1.1$ ($\rho = 39.9$ Mbps), the PLR value of both schemes goes up significantly in comparison with other load cases. Since all UEs under $\rho = 1.1$ have no chance at all to enter the sleep mode in virtual time, the both schemes have already reached the boundary condition in this case as displayed in Figure 13. Therefore, the high value of PLR for $\rho = 1.1$ is due to the saturation of the RT traffic load.
3. As shown in Figure 16, PLR of LBPS-Merge-RT is mostly higher than that of LBPS-Split-RT under DB = 6 ms. A very small DB value such as 6 ms makes fewer groups of RT UEs in both schemes. However, due to separation of RT UEs and NRT UEs in LBPS-Merge-RT, fewer groups of RT UEs mean that more RT UEs are grouped together in sleep scheduling, which creates more competition among RT packets in transmission and thus results in higher PLR of LBPS-Merge-RT. On the other hand, since LBPS-Split-RT mixes RT UEs and NRT UEs together in sleep scheduling and RT packets have priority over NRT packets in transmission, it also contributes to the lower PLR of LBPS-Split-RT than LBPS-Merge-RT. The situation of transmission competition among RT packets in LBPS-Merge-RT is lessened for a larger value of DB, such as 12 ms in Figure 17.

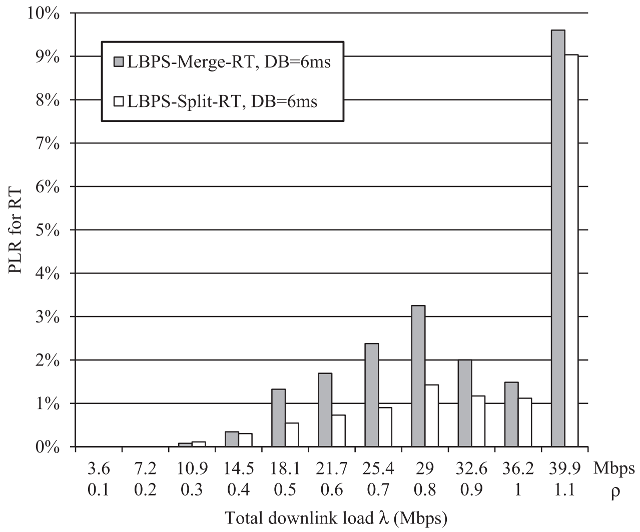

FIGURE 16 PLR for RT with DB = 6 ms in C3 (All-H UEs). DB, delay bound; LBPS, Load-Based Power Saving; PLR, packet loss ratio; RT, real-time; UE, user equipment

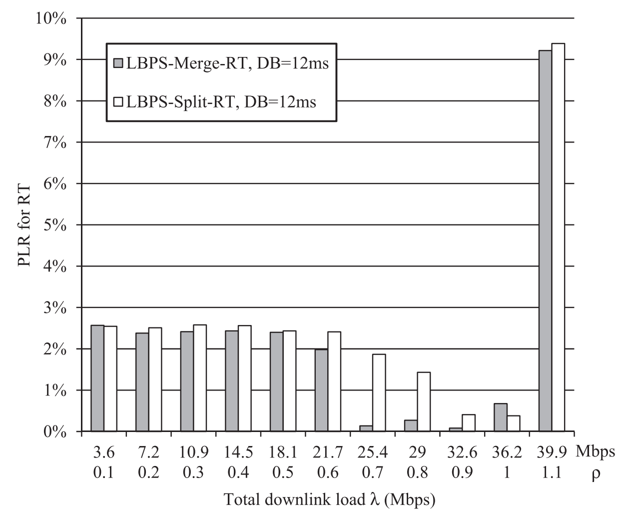

FIGURE 17 PLR for RT with DB = 12 ms in C3 (All-H UEs). DB, delay bound; LBPS, Load-Based Power Saving; PLR, packet loss ratio; RT, real-time; UE, user equipment

In summary, both LBPS-Split-RT and LBPS-Merge-RT can effectively support power saving for RT UEs and NRT UEs in the network, but LBPS-Merge-RT shows more flexibility in supporting RT UEs due to its ability of allowing different sleep cycle lengths in sleep scheduling.

5 | CONCLUSION

The issue of energy saving in modern communication system has long been an important research topic in the literature. The authors previously proposed the idea of LBPS and 3 LBPS schemes, namely, LBPS-Aggr, LBPS-Split, and LBPS-Merge, for the mode of FDD in LTE. In this paper, the applicability of the previously proposed schemes to the mode of TDD in LTE is investigated. The idea of virtual time associated with the mapping mechanism from virtual time to actual time in sleep scheduling is proposed. The following 3 types of mapping strategy are proposed in this paper: one-to-all mapping (M1), continuous mapping (M2), and one-to-one first mapping (M3). Theoretical analysis and simulation study show that M3 outperforms the other 2 in power saving efficiency.

With the help of the mapping mechanism, 3 revised LBPS schemes, namely, LBPS-Aggr-RT, LBPS-Split-RT, and LBPS-Merge-RT, are proposed to support power saving for RT UEs and NRT UEs in LTE-TDD. Simulation study demonstrates the benefit of the proposed schemes over the standard-based mechanism in of power saving efficiency. It also shows that LBPS-Split-RT and LBPS-Merge-RT can achieve better power saving efficiency than LBPS-Aggr-RT by separating UEs in different groups in sleep scheduling. Moreover, due to the flexibility of LBPS-Merge-RT to allow different sleep cycle lengths for UEs, it is concluded that LBPS-Merge-RT is better than LBPS-Split-RT in supporting the combination of RT UEs and NRT UEs in the network.

It is worth mentioning that the assumption of Poisson process for the arrival traffic limits the applicability of the LBPS schemes for more complicated traffic types, which leads to a direction of the future work in adopting a more sophisticated traffic model. Another direction of the future work is to consider the mobility and handover of UEs in designing sleep scheduling schemes.

ACKNOWLEDGEMENTS

This work was supported in part by the Ministry of Science and Technology, Taiwan, R.O.C., under grant no. MOST 104-2221-E-260-004.

REFERENCES

1. 3GPP TS 36.300. Evolved Universal Terrestrial Radio Access (E-UTRA) and Evolved Universal Terrestrial Radio Access Network (E-UTRAN), Rel. 8, v8.5.0, May 2008.
2. 3GPP TS 36.300. Evolved Universal Terrestrial Radio Access (E-UTRA) and Evolved Universal Terrestrial Radio Access Network (E-UTRAN), Rel. 10, v10.3.0, March 2011.
3. Chen S, Zhao J, Peng Y. The development of TD-SCDMA 3G to TD-LTE-advanced 4G from 1998 to 2013. *IEEE Wireless Communications*. 2014;21(6):167-176.
4. Chen S, Sun S, Wang Y, Xiao G, Tamrakar R. A comprehensive survey of TDD-based mobile communication systems from TD-SCDMA 3G to TD-LTE(A) 4G and 5G directions. *China Commun*. 2015;12(2):40-60.
5. Kim M, Kim S, Lim Y. An implementation of downlink asynchronous HARQ for LTE TDD system. Proceedings, IEEE Radio and Wireless Symposium (RWS), Santa Clara, CA; January 15-18, 2012:271-274.
6. Wang C, Hou X, Harada A, Yasukawa S, Jiang H. HARQ Signalling Design for Dynamic TDD system. Proceedings, 80th IEEE Vehicular Technology Conference (VTC Fall), Vancouver, BC; September 14-17, 2014:1-5.
7. Sheu S-T, Kuo K-H, Yang C-C, Sheu Y-M. A go-back-N HARQ time bundling for machine type communication devices in LTE TDD. Proceedings, IEEE Wireless Communications and Networking Conference (WCNC), Shanghai; April 7-10, 2013:280-285.
8. Lu Y, Liu L, Li M, Chen L. Uplink control for low latency HARQ in TDD carrier aggregation. Proceedings, 75th IEEE Vehicular Technology Conference (VTC Spring), Yokohama; May 6-9, 2012:1-5.
9. Malmirchegini M, Yenamandra R, Chaudhuri KR, Bautista JEV. Distributed and adaptive optimization of LTE-TDD configuration based on UE traffic type. Proceedings, 81st IEEE Vehicular Technology Conference (VTC Spring). Glasgow, Scotland; May 11-14, 2015:1-6.
10. Brown J, Khan JY. Performance analysis of an LTE TDD based smart grid communications network for uplink biased traffic. Proceedings, Globecom Workshops, Anaheim, CA; December 3-7, 2012:1502-1507.
11. Takahashi H, Yokomakura K, Imamura K. A transmit power control based interference mitigation scheme for small cell networks using dynamic TDD in LTE-advanced systems. Proceedings, 79th IEEE Vehicular Technology Conference (VTC Spring), Seoul, Korea; May 18-21, 2014;1-5.
12. Kini AV, Hosseinian M, Sadeghi P, Stern-Berkowitz J. A dynamic subframe set power control scheme for interference mitigation in reconfigurable TD-LTE systems. Proceedings, 23rd Wireless and Optical Communication Conference (WOCC), New Jersey, U.S.A.; May 9-10, 2014:1-6.
13. Yu B, Ishii H, Yang L. System level performance evaluation of dynamic TDD and interference coordination in enhanced local area architecture," Proceedings, 77th IEEE Vehicular Technology Conference (VTC Spring), Dresden; June 2-5, 2013:1-6.
14. Yu B, Yang L, Ishii H, Mukherjee S. Dynamic TDD support in Macrocell-assisted small cell architecture. *IEEE Journal on Selected Areas in Communications*. 2015;33(6):1201-1213.
15. Yang C-C, Mai Y-T, Chen J-Y, Shen Y-S, Kuo Y-C. LBPS: load-based power saving in the IEEE 802.16e network. *Computers and Electrical Engineering*. 2012;38(4):891-905.
16. Yang C-C, Chen J-Y, Mai Y-T, Liang C-H. Adaptive load-based and channel-aware power saving for non-real-time traffic in LTE. *EURASIP Journal on Wireless Communications and Networking*. 2015;2015(1):17.

How to cite this article: Yang C-C, Chen J-Y, Mai Y-T, Pan Z-Y. Integrated load-based power saving for real-time and nonreal-time traffic in LTE-TDD. *Int J Commun Syst*. 2017;e3299. https://doi.org/10.1002/dac.3299